Donor-Spiro-Acceptor Molecular Design: A Key Towards High-Efficiency Simplified Single-Layer Phosphorescent Organic Light-Emitting Diodes

Cyril Poriel, Joëlle Rault-Berthelot

Donor-*Spiro*-Acceptor Molecular Design: A Key Towards High-Efficiency Simplified Single-Layer Phosphorescent Organic Light-Emitting Diodes

Cyril Poriel and Joëlle Rault-Berthelot*

Univ Rennes, CNRS, ISCR-6226, F-35000 Rennes, France

Email: Cyril.poriel@univ-rennes1.fr

Table Of Content

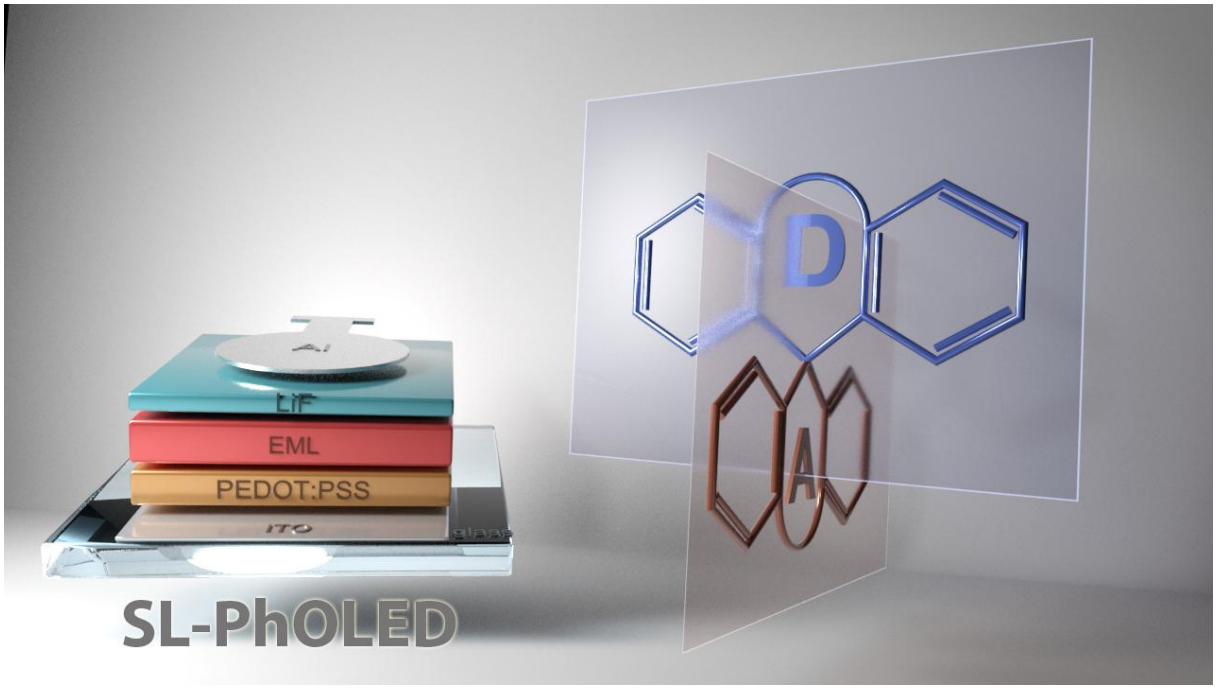

Conspectus

In organic electronic technologies, Single-Layer Phosphorescent Organic Light-Emitting Diodes (SL-PhOLEDs), only made of the electrodes and the Emissive Layer (EML), are a new generation of simplified PhOLEDs. In the field of OLED, such a type of devices has been studied for a long time as they represent 'ideal' devices. Indeed, simplifying the classical multi-layers structure of PhOLEDs (called ML-PhOLEDs) is important to reduce the amount of commodities, the manufacture complexity, the production and recycling costs. However, removing the functional organic blocking/transporting layers of a ML-PhOLED stack leads to an intense decrease of the PhOLED performance. This is the main problem; the researchers have faced in this field. To keep a high performance without the different organic layers, the effective injection, transport and recombination of charges in the device, should be performed by the EML and more particularly by the host materials. This host material should then display a set of electronic and physical properties, essential to reach a high-efficiency SL-PhOLED. However, reaching high performance SL-PhOLED is far more difficult than for ML-PhOLED and each molecular parameter of the host can dramatically decreases the PhOLED performance. The molecular design of the host is then crucial and a specific design has been particularly studied in the last years, which consists to link an electron-rich unit to an electron-poor unit *via* a spiro linkage. This design called Donor-*Spiro*-Acceptor (D-*Spiro*-A) allows to gather all the required properties in a single host and has allowed, these last years, important advances in the field. Nowadays, the most efficient SL-PhOLEDs use this molecular design and our group has particularly contributed to this research field. Thus, as the D-*Spiro*-A molecular design nowadays provides SL-PhOLEDs with the highest performance, well understanding its impact in the device efficiencies appears particularly important. This is the story we want to tell herein. In this account, we discuss

through a structure/properties/device performance relationship study (triplet state energy level, HOMO/LUMO energy levels, charge carriers mobilities, thermal and morphological properties and device performances), the recent advances made by this design in the field of SL-PhOLEDs. This account will mainly focus on the association of phenylacridine-like fragments (namely phenylacridine, indoloacridine, quinolinophenothiazine and quinolinoacridine) as electron rich unit and fluorene/phosphine oxide as electron-poor unit, which is, in the light of the literature, the combination, which has allowed the most important advances in the last years. Trying to unravel why this design has led to high performance, appears to be important for the future of SL-PhOLED technology, and may lead to new directions in term of molecular design.

Introduction

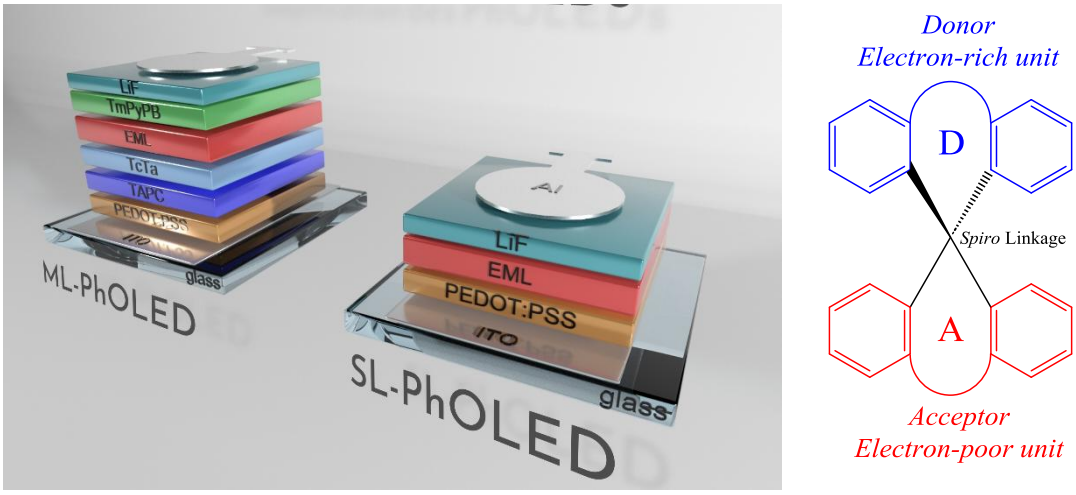

Figure 1. Left. Representation of the architecture of Multi-Layer (ML) and Single-Layer (SL)-PhOLEDs. Right. D-*Spiro*-A design. In the PhOLEDs, typical functional layers are presented, namely lithium fluorine (LiF) and poly(3,4-ethylenedioxythiophene)-poly(styrenesulfonate) (PEDOT-PSS) as hole- and electron-injecting layer respectively, di[4-(*N*,*N*-ditolyl-amino)-phenyl]cyclohexane (TAPC) and 1,3,5-tri[(3-pyridyl)-phen-3-yl]benzene (TmPyPB) as hole- and electron-transporting layer respectively and tris(4-(9*H*-carbazol-9-yl)phenyl)amine (TCTA) as exciton-confining layer.

Simplified OLEDs, with a reduced number of functional layers, have always interested researchers in order to decrease the complexity of the technology notably in term of manufacturing, Figure 1-left. The simplest devices, called Single-Layer OLED (SL-OLED), are only constituted of the Emissive layer (EML) and the electrodes, are easy to construct, and avoid interfacial phenomena often found in multi-layer stacks. However, removing the functional layers classically found in ML-OLEDs leads to a strong decrease of the device efficiency. For many years, researchers have tried to design high performance fluorescent[1] or phosphorescent EML[2] for this simplified technology but reaching high performance simplified devices remains a very difficult task.

To keep a high performance in Single-Layer Phosphorescent OLED (SL-PhOLED), the excellent injection, transport and recombination of charges in the device, should be performed by the EML. It should be first recall that the EML of a phosphorescent PhOLED is constituted by a heavy-metal organometallic complex emitter dispersed into an organic host to harvest both singlet and triplet excitons. The molecular design of the host is then highly important to reach a high performance. In recent years, a design has allowed spectacular improvements in SL-PhOLED performance. sThis design called Donor-*Spiro*-Acceptor (D-*Spiro*-A) is constructed on the association of an electron-rich unit and an electron-poor unit *via* a spiro linkage, Figure 1-right.

This design not only gathers all the necessary properties for an ideal host for SL-PhOLED but allows as well an easy control of the electronic properties by a simple connection of a donor and an acceptor

unit *via* a spiro bridge. In principle, the versatility of this design is high as many donors or acceptors can be introduced to tune the properties (strength of the donor/acceptor combination, mobility, thermal stability…). The D-*Spiro*-A design has been broadly used, for the last 15 years, in the design of host materials for Multi-layer OLED either phosphorescent[3-9] or Thermally Activated Delayed Fluorescent,[10-15] but its story in SL-PhOLEDs has only started several years later.

Three key properties can be fixed by this design: the HOMO and LUMO levels, the E_T and the thermal properties. The HOMO/LUMO levels of a host are particularly important as they notably determine the threshold voltage (V_{on}), a key property in SL-PhOLED. In the D-*Spiro*-A design, there is a complete HOMO/LUMO separation thanks to the spiro bridge. Therefore, their energies are fixed by the donor and by the acceptor moieties respectively. This design also allows controlling the E_T, which is always fixed by the less conjugated molecular unit. The most efficient materials presented in this account are constructed on a fluorene substituted by electron-accepting phosphine oxide units. In these examples, the E_T is fixed by the fluorene, which presents an E_T of 2.92 eV.[16] Finally, this design, thanks to its spiro-bridge, allows maintaining excellent thermal and morphological stabilities, a key feature for evaporation processes and device stability. Thus, the spiro-bridge has a double key role: (i) interrupting the electronic coupling between the two spiro-connected cores and (ii) achieving a high thermal/morphological stability.

This account will focus on the recent advances made in the field of SL-PhOLEDs thanks to the D-*Spiro*-A design. Through a structure/properties/device performance relationship study, the importance of this design on the photophysical, electrochemical, thermal and charge transport properties and the link with the SL-PhOLEDs performance will be discussed. We aim providing guidelines for the future design of hosts for SL-PhOLEDs. As the association of phenylacridine-like fragment (namely phenylacridine, indoloacridine, quinolinoacridine and quinolinophenothiazine) as donor and fluorene/phosphine oxide fragments as acceptor has appeared, in recent years, as one of the most efficient combination for SL-PhOLEDs, this association is the main topic of this account (Figure 2).

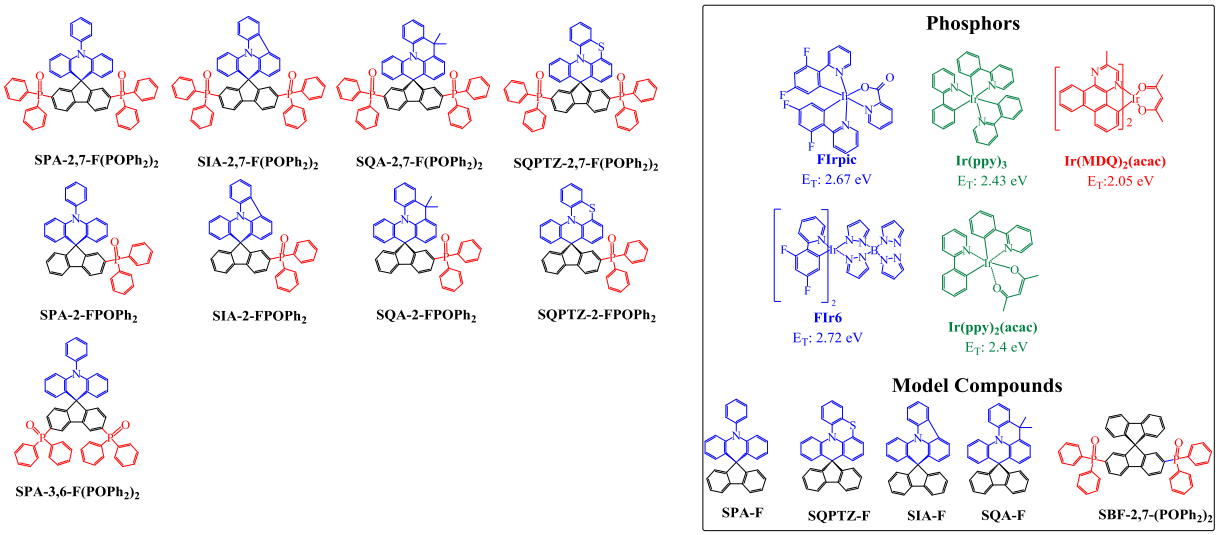

Figure 2. Donor-*Spiro*-Acceptor hosts used in SL-PhOLEDs (model compounds and phosphors also presented).

Understanding the D-*Spiro*-A design and its relevancy for SL-PhOLEDs: the phenylacridine/fluorene diphenylphosphine oxide combination

The first important step in the development of the D-*Spiro*-A design for SL-PhOLEDs was to compare its properties to corresponding D and A building blocks in order to define the relevancy of the association. In 2020, our group has synthesized a host called **SPA-2,7-F(POPh$_2$)$_2$** (spirophenylacridine-2,7-(diphenylphosphine oxide)-fluorene)[17] built on the combination of an electron-rich unit, namely phenylacridine[7, 8] and an electron-poor unit, namely 2,7-(diphenylphosphine

oxide)-fluorene. This host appeared to be very efficient when incorporated in green and more importantly in blue PhOLEDs. It should be reminded that blue emission has concentrated many researches for the last twenty years and particularly in organic optoelectronics. Despite the fantastic advances made, reaching high-efficiency and stable blue OLEDs is still an important challenge for the next step.[1, 2, 18-20] High performance blue SL-PhOLEDs are then particularly challenging.

The fundamental understanding of the properties of **SPA-2,7-F(POPh$_2$)$_2$** and its link with the high SL-PhOLED performance reached was an important milestone in our development of hosts for SL-PhOLEDs. Two model compounds (Figure 2) combining either the electron-rich function (spirophenylacridine-fluorene **SPA-F**) or the electron-poor function (9,9'-spirobi[fluorene]-2,7-diylbis(diphenylphosphine oxide)), **SBF(POPh$_2$)$_2$**) have been thus synthesized and studied in order to find out about the incorporation of the electron-rich/electron-poor units in **SPA-2,7-F(POPh$_2$)$_2$**.[17] This work has driven the further designs investigated in our group as presented below. Thus, the cyclic voltammetries (Figure 3) show that **SPA-2,7-F(POPh$_2$)$_2$** displays a first oxidation/reduction wave at very similar potentials than those of its building units **SPA-F/SBF(POPh$_2$)$_2$** (HOMO **SPA-2,7-F(POPh$_2$)$_2$/SPA-F**: -5.33/-5.26 eV; LUMO **SPA-2,7-F(POPh$_2$)$_2$/SBF(POPh$_2$)$_2$**: -2.55/-2.55 eV). This shows that the first electron transfer is respectively centred on the acridine unit in oxidation and on the 2,7-(diphenylphosphine oxide)-fluorene fragment in reduction in accordance with the HOMO/LUMO localization (HOMO spread out on the acridine and LUMO on the fluorene, Figure 3, top-inset). This rational design leads to a gap contraction of **SPA-2,7-F(POPh$_2$)$_2$** (2.78 eV) compared to the two model compounds (**SPA-F**: 3.39 eV, **SBF(POPh$_2$)$_2$**: 3.54 eV).[21] This is a central piece in this design as both types of charges should be injected and transported.

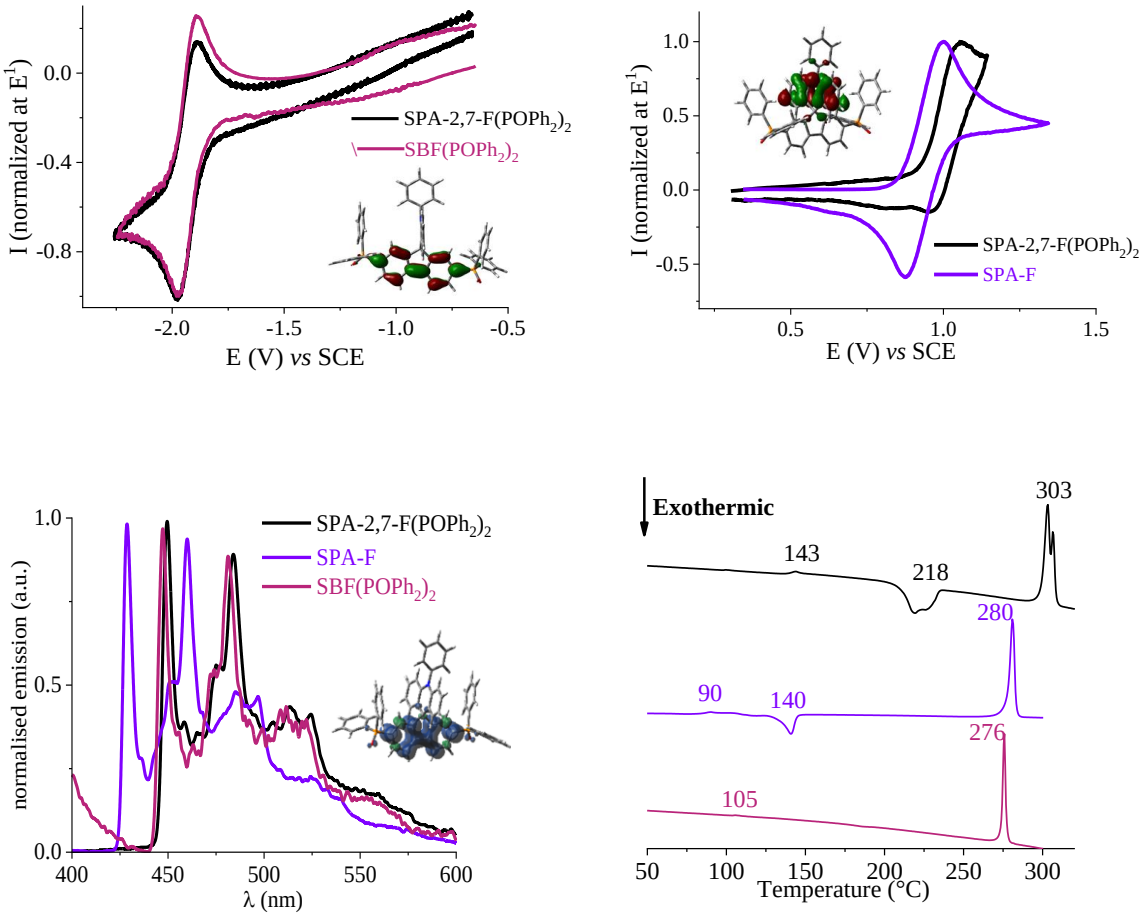

Figure 3. **SPA-2,7-F(POPh$_2$)$_2$**, **SBF(POPh$_2$)$_2$** and **SPA-F**. Top. Normalized cyclic voltammograms in the cathodic (left, DMF+BuN_4PF_6 0.1M) or the anodic (Right, CH_2Cl_2+Bu_4NPF_6 0.2M) range. Sweep-rate of 100

$mV.s^{-1}$, platinum disk working electrode. Inset: Representations of HOMO and LUMO orbitals for **SPA-2,7-F(POPh$_2$)$_2$** obtained by DFT. Bottom. Emission spectra at 77K (Left, 2Me-THF) and Differential Scanning Calorimetry traces (Right, 2nd heating). Inset. SDD of **SPA-2,7-F(POPh$_2$)**.

Understanding the optical properties and particularly the E_T was also an important step. Herein, the E_T was easily controlled by the less conjugated fragment. This has been shown by the overlay of the phosphorescence spectra of **SBF(POPh$_2$)$_2$** and **SPA-2,7-F(POPh$_2$)$_2$** (whereas **SPA-F** displays a blue shifted spectra). Thus, a high E_T of 2.76 eV was measured for both **SBF(POPh$_2$)$_2$** and **SPA-2,7-F(POPh$_2$)$_2$**, fully driven by the 2,7-(diphenylphosphine oxide)-fluorene fragment and independent of the donor unit (Figure 3, bottom-left). Theoretical calculations on **SPA-2,7-F(POPh$_2$)$_2$** showed that the spin density distribution (SDD) of the triplet state is fully located on the diphenylphosphine oxide-fluorene in accordance with the experimental data. However, it should be noted that the E_T is decreased compared to that of unsubstituted **SBF** (2.86 eV[22]). Oppositely to the two model compounds, **SPA-2,7-F(POPh$_2$)$_2$** does not present any fluorescence and only the phosphorescence is detected. This caused by the almost nul quantum yield at room temperature (<0.01), which should favoured the intersystem crossing between S_1 and T_1 leading to an intense phosphorescence at 77K.[6, 23]

The D-*Spiro*-A design also has considerable advantages in term of thermal properties, a key consideration for OLEDs. Indeed, thanks to the rigid spiro-linkage and bulky diphenylphosphine oxides, **SPA-2,7-F(POPh$_2$)$_2$** displays high decomposition temperature, T_d ca 474°C, and a high glass transition temperature, T_g of 143°C (Figure 3, bottom-right). The thermal and morphological features of **SPA-2,7-F(POPh$_2$)$_2$** are much improved over the two building units **SPA-F** and **SBF(POPh$_2$)$_2$**, which present a lower T_d (286 and 382°C respectively) and T_g (90 and 105°C respectively).

In a SL-PhOLED, because the charge carrier transporting and blocking layers have been supressed, balanced hole and electron mobilities are mandatory to promote effective recombination of carriers in the EML. This is even the most difficult obstacle to cross. Interestingly, **SPA-2,7-F(POPh$_2$)$_2$** also presents the transport properties of the two model compounds **SPA-F** and **SBF(POPh$_2$)$_2$** (μ_h/μ_e of 8.2×10^{-6} / 2×10^{-4} cm^2 V^{-1} s^{-1} for **SPA-2,7-F(POPh$_2$)$_2$** and μ_h of 1×10^{-5} cm^2 V^{-1} s^{-1} for **SPA-F** and μ_e of 6.9×10^{-5} cm^2 V^{-1} s^{-1} for **SBF(POPh$_2$)$_2$**). In addition, the mobilities of **SPA-2,7-F(POPh$_2$)$_2$** are also relatively well balanced with a ratio of the mobility μ_e / μ_h of only 24, which is excellent to maximize the recombination of hole and electron in the EML. Indeed, in SL-PhOLEDs, the absence of functional transporting layer imposes to have an EML with a ratio of the mobility close to one. Controlling this data is nevertheless highly difficult in term of material design. However, in this study, we only measured the mobilities of the host and we did not considered the phosphor in the charge transport, which has nevertheless a key importance as shown several years later.[24] We will discuss this feature in the last part of this account.

SPA-2,7-F(POPh$_2$)$_2$ used as host in a PhOLED with FIrpic as emitter displayed a very high EQE of 18%, a CE of 39 cd/A and a PE of 38.4 lm/W (0.04 mA/cm²). This result was particularly impressive since benchmark blue SL-PhOLEDs with model compounds **SPA-F** and **SBF(POPh$_2$)$_2$** as host displayed extremely low performances (EQE<1%). As far as we know, **SPA-2,7-F(POPh$_2$)$_2$** is still today the second most efficient blue SL-PhOLED ever reported (the most efficient host in blue SL-PhOLED has been reported in 2014, EQE=20.3%[25]). Similarly, in green $Ir(ppy)_3$ SL-PhOLEDs, the performance obtained was also high with an EQE_{max} reaching 16.4%, and corresponding CE of 56.3 cd/A and PE of 53.6 lm/W. Due to the short HOMO/LUMO gap, the V_{on} was low, 2.3 V, translating a very efficient injection of the charges. Finally, in red PhOLEDs, EQE_{max} of 8.7% was reached with $Ir(MDQ)_2(acac)$ as dopant showing the possible use of **SPA-2,7-F(POPh$_2$)$_2$** as universal host in PhOLEDs (see below).

This work has shown that **SPA-2,7-F(POPh$_2$)$_2$** provides a rational combination of the models' properties with nevertheless significantly improved devices performances. This work has driven our future designs.

In the light of the performance reached, we decided to modify the number and the position of the phosphine oxides in order to increase the E_T. We were aware that these modifications would have important consequences on the LUMO energy level and the charge carriers but this was a mandatory step to find out, which parameters were the most important in the device performance. Thus, two other

structurally related hosts, **SPA-3,6-F(POPh$_2$)$_2$** and **SPA-2-FPOPh$_2$** were synthesized.[21] In **SPA-2-FPOPh$_2$** and in **SPA-2,7-F(POPh$_2$)$_2$** the phosphine oxide(s) was (were) located in *para* positions of the biphenyl core of the fluorene (C2 and C7 positions) whereas in **SPA-3,6-F(POPh$_2$)$_2$**, they were located in *meta* position (C3 and C6 positions). Oppositely to C2/C7 positions, widely developed in fluorene chemistry,[26] C3/C6 positions have only been investigated recently.[16, 26, 27] The *meta*-substitution provides an electronic decoupling whereas the *para*-substitution extends the conjugation. This property has been, beneficially used to increase the E_T of host materials.[27-29]

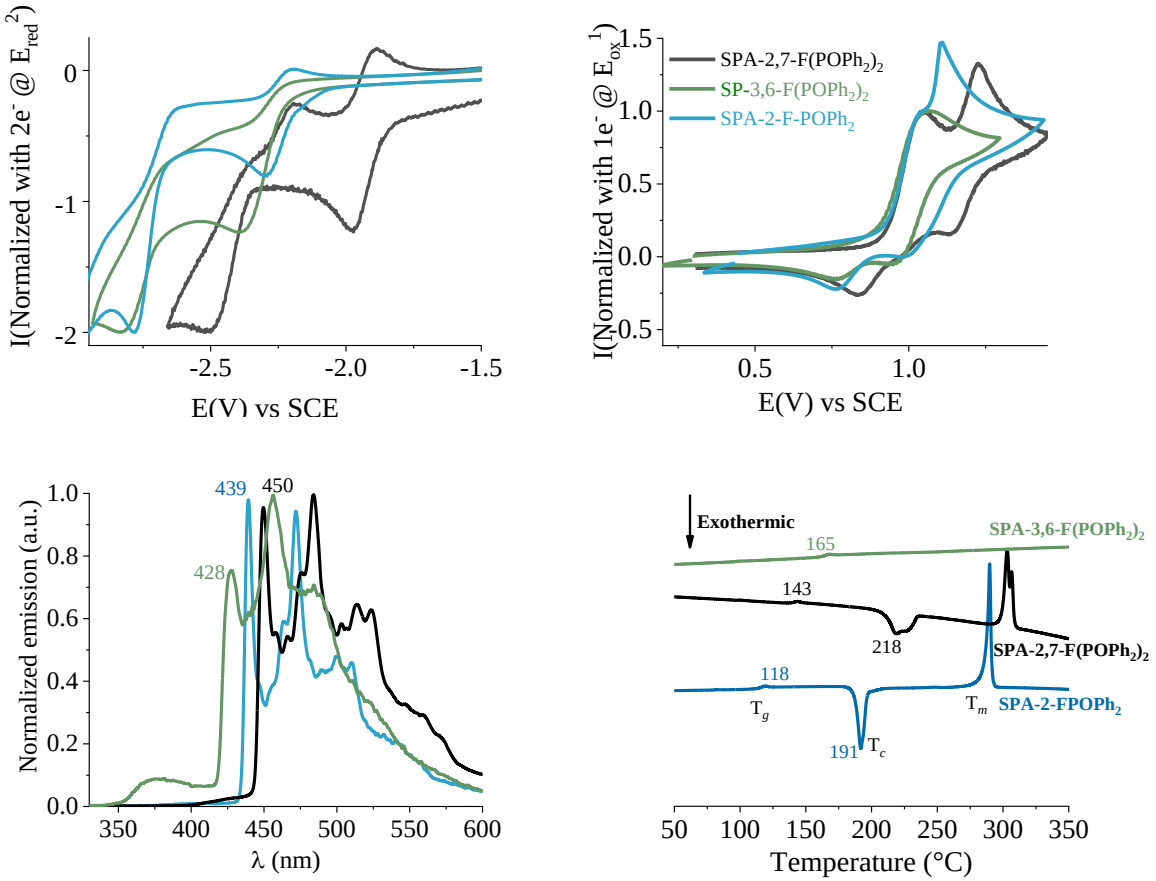

Figure 4. SPA-2,7-F(POPh$_2$)$_2$, SPA-3,6-F(POPh$_2$)$_2$ and **SPA-2-FPOPh$_2$**. Top. Normalized cyclic voltammograms in the cathodic (Left, DMF+BuN_4PF_6 0.1 M) or the anodic (Right, CH_2Cl_2+Bu_4NPF_6 0.2M) range. Sweep-rate: 100 mV.s^{-1}, platinum disk working electrode. Bottom. Emission spectra at 77K (Left, 2Me-THF) and Differential Scanning Calorimetry traces (Right, 2nd heating).

The HOMO levels have been measured at similar energies, -5.33 eV, for both **SPA-2,7-F(POPh$_2$)$_2$** and **SPA-2-FPOPh$_2$** and -5.31 eV for **SPA-3,6-F(POPh$_2$)$_2$** translating a first oxidation on the phenylacridine unit for the three compounds. The LUMO levels have respectively been evaluated at -2.55 eV, -2.23 eV and -2.18 eV for **SPA-2,7-F(POPh$_2$)$_2$**, **SPA-2-FPOPh$_2$** and **SPA-3,6-F(POPh$_2$)$_2$**. Thus, the LUMOs displayed a different behaviour as located on the acceptor fragment and assigned to both the number and the position of the diphenylphosphine oxide units. The shift of the phosphine oxides from C2/C7 in **SPA-2,7-F(POPh$_2$)$_2$** to C3/C6 in **SPA-3,6-F(POPh$_2$)$_2$** leads to an increase of the LUMO level (-2.55 vs -2.18 eV) due to the decoupling between the phosphine oxide (which decreases its electron accepting effect) and the fluorene in the latter.[16, 26] With only one phosphine oxide attached at C2, the LUMO of **SPA-2-FPOPh$_2$** (-2.23 eV) is higher than that of **SPA-2,7-F(POPh$_2$)$_2$** (-2.55 eV). Thus, the HOMO/LUMO gap can be easily tuned by the number and the position of the phosphine oxides. In addition, the strategy to shift the phosphine oxides in C3/C6 or to remove one of them significantly increases the E_T from 2.76 eV in **SPA-2,7-F(POPh$_2$)$_2$**, to 2.82 eV in **SPA-2-F(POPh$_2$)** and to 2.90 eV in **SPA-3,6-F(POPh$_2$)$_2$**. This shows how all the electronic properties can be tuned in this design. The position and the number of phosphine oxides also determine the

thermal and morphological stability as shown Figure 4 (Bottom-right). The T_g is much increased (143°C) when two phosphine oxides are attached at C3/C6.

Despite these promising properties and particularly a high E_T, the sky blue (FIrpic) SL-PhOLEDs with either **SPA-3,6-F(POPh$_2$)$_2$** (EQE=6.5% and V_{on}=3.5 V) or **SPA-2-FPOPh$_2$** (EQE=8.6% and V_{on}=2.8 V) have revealed lower performance than those of **SPA-2,7-F(POPh$_2$)$_2$** (EQE=18% and V_{on}=2.5 V). This shows that the E_T is not the main parameter involved in the performance. The lower device efficiencies obtained with **SPA-3,6-F(POPh$_2$)$_2$** and **SPA-2-FPOPh$_2$** have been assigned to a combination of several factors: gap extension leading to an increase of the V_{on}, higher LUMO level less adapted to the LUMO of FIrpic (-2.52 eV),[21] lower and less balanced mobility of charge carriers. Indeed, the shift or removal of phosphine oxide units also has important repercussions on the charge transport. **SPA-2,7-F(POPh$_2$)$_2$** presents the highest mobility both in hole and in electron and the most balance charge transport (μ_h/μ_e **SPA-2,7-F(POPh$_2$)$_2$**: 8.2×10^{-6} / 2×10^{-4} cm^2 V^{-1} s^{-1}, **SPA-2-FPOPh$_2$**: 1.9×10^{-7} / 1.3×10^{-5} cm^2 V^{-1} s^{-1} and **SPA-3,6-F(POPh$_2$)$_2$**: 1.4×10^{-8} and 3.1×10^{-6} cm^2 V^{-1} s^{-1}). The charge balance is undoubtedly an important consideration in SL-PhOLED to avoid a shift of the recombination zone close to the metal electrodes, which usually leads to excitons quenching. However, at that time, we did not consider the whole EML (host + emitter) for the charges transport measurements but only the host material. This was not sufficient to have a precise view of the charges transport as will be shown later.

The high E_T of both **SPA-3,6-F(POPh$_2$)$_2$** and **SPA-2-FPOPh$_2$** has then allowed to consider them with an emitter displaying shorter wavelength than FIrpic, namely FIr6. This phosphor has a blue shifted emission spectrum compared to FIrpic (λ=463, 491 nm for FIr6 *vs* 473, 497 nm for FIrpic) and could be a first step towards deep blue SL-PhOLEDs[21] absent, at that time, from literature (note that FIr6 has previously been studied in ML-PhOLEDs[30, 31]). Surprisingly, this time, the highest performance was reached with **SPA-2-FPOPh$_2$** with an EQE of 9.1%,[21] the two other hosts displaying lower EQE of 6.5%. It is interesting to note that the performance of **SPA-2,7-F(POPh$_2$)$_2$** with FIr6 was low especially when compared to that with FIrpic (6.5 *vs* 18%), clearly showing that the host/guest combination is more important than the host itself. In 2022, we have provided several studies discussing the importance of the host/guest combination on the charge transport.[24] They are detailed below.

These materials have also been used in green and red PhOLEDs, showing their universal behaviour. In both red and green PhOLEDs, **SPA-2,7-F(POPh$_2$)$_2$** was always the most efficient host, showing the versatility and the high potential of this host as universal material (green/red PhOLEDs: EQE=16.4/8.7, 13.9/5.3 and 10.4/4.5% for **SPA-2,7-F(POPh$_2$)$_2$**, **SPA-3,6-F(POPh$_2$)$_2$** and **SPA-2-FPOPh$_2$** respectively). These performances were undoubtedly promising for a series of structurally related hosts, releasing the efficiency of this design.

What have been learned from this first series of results? First, high performance SL-PhOLEDs can be reached with D-*Spiro*-A host design and this was a key feature to carry on. However, in the light of the performance obtained with **SPA-2-FPOPh$_2$**, it remained difficult to define precise guidelines for the future. Indeed, the performance of this host was very modest except with FIr6, which is a challenging phosphor. Thus, E_T, HOMO/LUMO energy levels and mobilities were all key factors in the SL-PhOLED performance and it was hard to discriminate one among the others. This is the main difficulty of the design of host materials for SL-PhOLEDs. At that time, we were nevertheless convinced that a good balance of charges was a central feature to reach highly efficient SL-PhOLEDs.

Modification of the electron-rich unit (Phenylacridine-like fragments): a tool to modulate the electronic properties

Driven by these convincing results, and particularly those of **SPA-2,7-F(POPh$_2$)$_2$**, we designed, in 2021, new D-*Spiro*-A hosts. We decided to keep the fluorene diphenylphosphine oxide unit in place in order to insure an efficient electron transport (in this field, the electron transport is always an issue) and we modified the electron-rich unit. This modification should impact the HOMO energy level and

the hole mobility but should maintain the other properties and particularly the thermal stability. In the field of OLEDs, the widely known electron-rich phenylacridine unit (PA)[7, 32] used in **SPA-2,7-F(POPh$_2$)$_2$** holds a special place as it is one of the most efficient building unit due to its excellent charges injection/transport properties.[7, 14, 17, 33] This fragment has been, in recent years, a fantastic playground for organic chemists, which have designed other structurally related fragment, named IndoloAcridine (IA),[4, 34, 35] QuinolinoPhenoThiaZine (QPTZ),[6, 36] and QuinolinoAcridine (QA)[13, 37] (Figure 5), which all display specific electronic properties. In these new hosts, the two phenyl rings of the PA backbone are connected in a different manner and all the properties originate from this structural feature. Thus, in indolocacridine (IA), the linkage is a carbon-carbon bond whereas in quinolinophenothiazine (QPTZ) and quinolinoacridine (QA), the linkage is either a sulphur or a carbon bridge respectively (Figure 5). These building units have successfully been incorporated in ML-PhOLEDs[4, 6, 34] and in TADF OLEDs[13, 37-39] but remained unknown in SL-PhOLEDs.

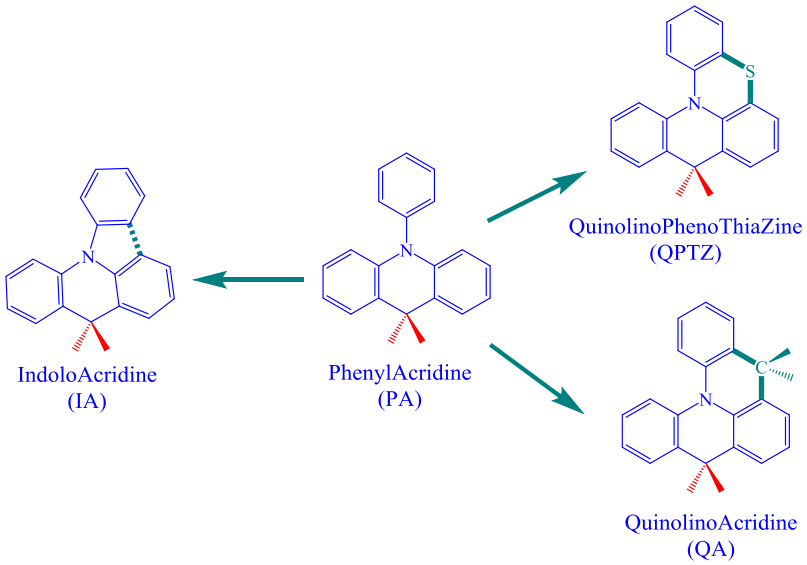

Figure 5: Phenylacridine (PA), indoloacridine (IA), quinolinophenothiazine (QPTZ) and quinolinoacridine (QA) fragments.

Thus, we synthesized three D-*Spiro*-A hosts, spiroquinolinophenothiazine-2,7-bis(diphenylphosphine oxide)-fluorene (**SQPTZ-2,7-F(POPh$_2$)$_2$**),[40] spiroquinolinoacridine-2,7-bis(diphenylphosphine oxide)-fluorene (**SQA-2,7-F(POPh$_2$)$_2$**)[41] and spiroindoloacridine-2,7-bis(diphenylphosphine oxide)-fluorene (**SIA-2,7-F(POPh$_2$)$_2$**)[42] (Figure 2) to evaluate their potentials in SL-PhOLEDs. The results obtained in SL-PhOLEDs confirmed us the difficulty to design a high performance host with well-defined design guidelines.

For the three hosts, the LUMOs, fixed by the acceptor are almost identical (ca -2.5/-2.6 eV) but the HOMOs, fixed by the donor, are all different, -5.25 eV for **SQPTZ-2,7-F(POPh$_2$)$_2$**), -5.32 eV for **SQA-2,7-F(POPh$_2$)$_2$** and -5.59 eV for **SIA-2,7-F(POPh$_2$)$_2$**. The gap can be therefore easily tuned by the strength of the donor unit. Compare to its PA counterpart **SPA-2,7-F(POPh$_2$)$_2$** (-5.33 eV), the QPTZ fragment presents a significant increase of the HOMO level and stable radical cations (Figure 6, top-right), an interesting feature for SL-PhOLEDs.[6] Oppositely, the IA fragment displays a lower HOMO level compare to its PA analogue, as previously observed in literature for other systems.[4, 34] The strong electron-rich character of QPTZ is due to the electron-donating behaviour of the intracyclic sulphur atom, which drives the HOMO level (Figure 6, top-right, bottom-right).[6] The QA fragment, with its C(Me)$_2$ bridge displays an intermediate behaviour as the HOMO of **SQA-2,7-F(POPh$_2$)$_2$** is nearly identical to that of **SPA-2,7-F(POPh$_2$)**, indicating the weak electronic effect of a carbon atom (Figure 6, top-right, bottom-right). In addition to this HOMO/LUMO gap modulation, the efficiency of this design holds in the possibility to keep the E_T very high as it is fixed by the fluorene fragment. Indeed, the E_T of the three hosts are identical to that of **SPA-2,7-F(POPh$_2$)$_2$**, ie 2.76 eV, discussed

above. Thus, the donor does not influence this data, which remains high and in accordance with RGB phosphors.

The charge carriers mobilities were also significantly modified by the nature of the donor, **SIA-2,7-F(POPh$_2$)$_2$**: $\mu_e=5\times10^{-8}$ $cm^2.V^{-1}.s^{-1}$/$\mu_h=1.1\times10^{-4}$ $cm^2.V^{-1}.s^{-1}$, $\mu_e/\mu_h=4.5\times10^{-4}$, **SQA-2,7-F(POPh$_2$)$_2$**: $\mu_e=9.5\times10^{-5}$ $cm^2.V^{-1}.s^{-1}$/$\mu_h=1.3\times10^{-5}$ $cm^2.V^{-1}.s^{-1}$, $\mu_e/\mu_h=7.3$ and **SQPTZ-2,7-F(POPh$_2$)$_2$**: $\mu_e=1\times10^{-3}$ $cm^2.V^{-1}.s^{-1}$/$\mu_h=1.3\times10^{-5}$, $\mu_e/\mu_h=77$). Thus and despite the similarity between the molecular structures, until 4 orders of magnitude were measured for the different mobilities (measured in similar conditions) demonstrating the huge impact of the donor on both hole and electron mobilities due to the different intermolecular stacking. But the most surprising feature was highlighted when incorporated in SL-PhOLEDs as all the hosts have displayed significantly lower performance than those of **SPA-2,7-F(POPh$_2$)$_2$**. Indeed, in the light of previous works, we believed that **SQA-2,7-F(POPh$_2$)$_2$** would be the most efficient in SL-PhOLED due to its excellent charge balance (7.3). However, all the EQE measured, either in red (Ir(MDQ)$_2$acac, 5.6%), green (Ir(ppy)$_2$acac, 8.9%) and blue (FIrpic, 10.0%) were surprisingly low and below (or slightly above) those of **SQPTZ-2,7-F(POPh$_2$)$_2$**) (Ir(MDQ)$_2$acac: 8.4%, Ir(ppy)$_2$acac: 11.3%, FIrpic: 8.4%), for which the charges were less balanced. The charge balance of **SQPTZ-2,7-F(POPh$_2$)$_2$** was indeed 10 times less balanced than that of **SQA-2,7-F(POPh$_2$)$_2$**. The EQE measured for **SIA-2,7-F(POPh$_2$)$_2$**, for which the charges are strongly unbalanced ($\mu_h/\mu_e=2200$) were also low (8.0% with Ir(MDQ)$_2$acac, 6.9% with Ir(ppy)$_2$acac and 7.3% with FIrpic,). These results have allowed us to reconsider the importance of the mobility of the charge carriers in the SL-PhOLEDs performance or more precisely the way it should be considered. This will be discussed in the last part.

However, **SQPTZ-2,7-F(POPh$_2$)$_2$** has presented several interesting properties assigned to the QPTZ fragment.[40] This host notably displayed high luminances (10000 cd/m^2 for blue and red and 40000 cd/m^2 for green SL-PhOLEDs). These luminances were higher than those of **SPA-2,7-F(POPh$_2$)$_2$**, (which were the highest reported at that time) and have highlighted the simportance of the QPTZ core in such devices. This means that **SQPTZ-2,7-F(POPh$_2$)$_2$** based SL-PhOLEDs can support a higher current density than those based on **SPA-2,7-F(POPh$_2$)$_2$**. The QPTZ fragment, due to its high HOMO energy level, also allowed decreasing the threshold voltage, a fundamental feature in 'single-layer' technology.

The origin of the high luminance of **SQPTZ-2,7-F(POPh$_2$)$_2$** can be related to the excellent thermal properties of this material. Indeed, **SQPTZ-2,7-F(POPh$_2$)$_2$** presents a higher Tg (169°C) than **SPA-2,7-F(POPh$_2$)$_2$** (143°C), Figure 6, bottom-left. This has been correlated to the incorporation of a bridged atom, which rigidifies the structure compared to **SPA-2,7-F(POPh$_2$)$_2$**, improving as well the thermal properties. This characteristic was also found in **SQA-2,7-F(POPh$_2$)$_2$** , with it CMe_2 bridge highlighting the beneficial effect of a bridging atom on the thermal properties. The crystallization temperature T_c at ca. 218°C found for **SPA-2,7-F(POPh$_2$)$_2$** is also interestingly suppressed in both **SQPTZ-2,7-F(POPh$_2$)$_2$** and **SQA-2,7-F(POPh$_2$)$_2$**. As amorphous materials are required in OLEDs, this is an important property of the QPTZ fragment.

Despite some interesting devices performances were obtained with **SQPTZ-2,7-F(POPh$_2$)$_2$**,[40] this series of C2/C7 di-substituted fluorene hosts has globally provided disappointed performance in SL-PhOLEDs particularly compared to that initially obtained with **SPA-2,7-F(POPh$_2$)$_2$**. The link between the charge transport and the SL-PhOLED efficiency was particularly unclear.

We then decided to remove one phosphine oxide fragment to fit with high E_T phosphors such as FIr6 and to carefully study the charge transport but this time in a different way, considering the whole EML (host and emitter). This is detailed below.

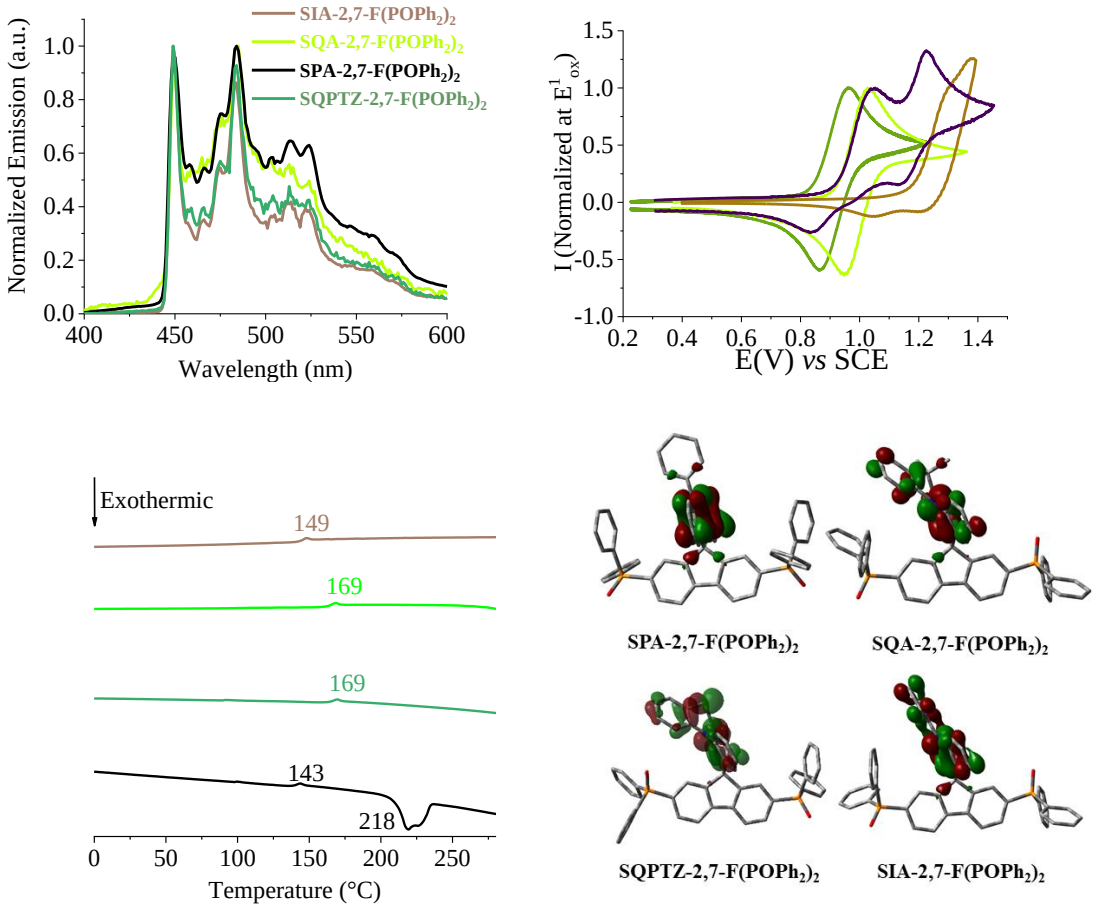

Figure 6. **SIA-2,7-F(POPh$_2$)$_2$**, **SQA-2,7-F(POPh$_2$)$_2$** and **SQPTZ-2,7-F(POPh$_2$)$_2$** Top. Normalized emission spectra at 77K in 2-MeTHF (λ_{exc}=310 nm, Left), Normalized cyclic voltammograms (CH_2Cl_2+Bu_4NPF_6 0.2M) range. Sweep-rate: 100 mV.s^{-1}, platinum disk working electrode (Right). Bottom. Differential Scanning Calorimetry traces (Left, 2nd heating), Representations of HOMO orbitals obtained by DFT in B3LYP/6-311+G(d,p) (Right).

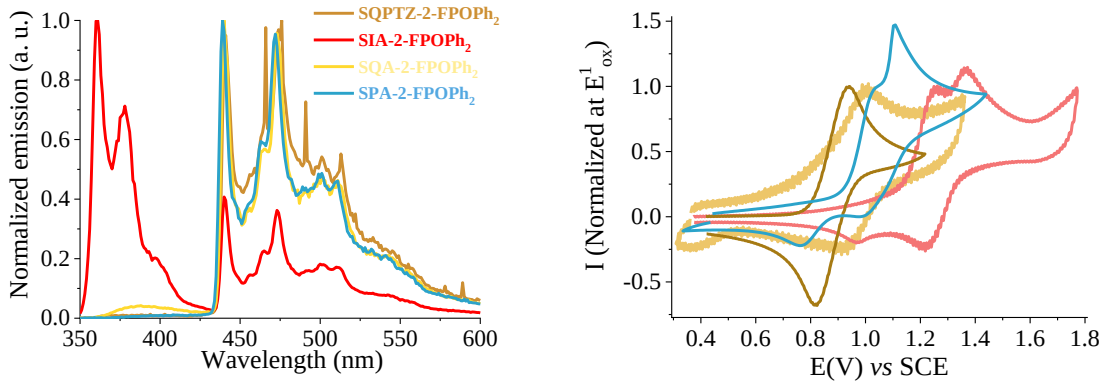

Figure 7. **SIA-2-FPOPh$_2$**, **SQA-2-FPOPh$_2$**, **SPA-2-FPOPh$_2$** and **SQPTZ-2-FPOPh$_2$** Left. Normalized emission spectra at 77K in 2-MeTHF (λ_{exc}=310 nm). Right. Normalized cyclic voltammograms (CH_2Cl_2+Bu_4NPF_6 0.2M) range. Sweep-rate: 100 mV.s^{-1}, platinum disk working electrode.

Thus, several years later, the four different donors described above were connected to the 2-fluorene-phosphine oxide unit in **SPA-2-FPOPh$_2$** (already presented in Part 1), **SQPTZ-2-FPOPh$_2$**, **SIA-2-**

FPOPh$_2$ and **SQA-2-FPOPh$_2$** in order to increase the E_T and to provide a precise structure/properties/device performance map. As we learned above, the E_T is fixed by the fluorene/phosphine oxide fragment and was then measured identical for the four hosts. Therefore, the four hosts displayed a very high E_T of 2.82 eV (Figure 7, left) allowing their use with FIr6. These four materials present nevertheless different fluorescent contributions showing the different impact of the donor on S_1 and T_1 excited state (Figure 7, left). This feature provides an interesting way of S_1 and T_1 tuning. As expected, the LUMOs were maintained similar, -2.23, -2.24, -2.31, - 2.26 eV for **SPA-2-FPOPh$_2$**, **SIA-2-FPOPh$_2$**, **SQA-2-FPOPh$_2$**, **SQPTZ-2-FPOPh$_2$** respectively, but were nevertheless slightly influenced by the spiro-connected electron-rich fragment (spiro-conjugation). The HOMOs, fixed by the donor, were all different but similar to the C2/C7 analogue described above, -5.33, -5.53, -5.31, -5.20 eV for **SPA-2-FPOPh$_2$**, **SIA-2-FPOPh$_2$**, **SQA-2-FPOPh$_2$**, **SQPTZ-2-FPOPh$_2$** respectively. The weaker electron-withdrawing effect of the 2-fluorene-diphenyl-phosphine oxide unit compare to the 2,7-fluorene-bis-diphosphine oxide units, increase the HOMO energy level of this series of molecules compare to their disubstituted analogues exposed above (except for phenylacridine derivatives for unknown reasons).

Again, the charge transport of these hosts were drastically different with huge differences as a function of the donor fragment, translating very different supramolecular arrangements (**SPA-2-FPOPh$_2$**: $\mu_e=1.3\times10^{-5}$ $cm^2.V^{-1}.s^{-1}/\mu_h=1.9\times10^{-7}$ $cm^2.V^{-1}.s^{-1}$, $\mu_h/\mu_e=1.5\times10^{-3}$, **SIA-2-FPOPh$_2$**: $\mu_e=8.5\times10^{-8}$ $cm^2.V^{-1}.s^{-1}/\mu_h=1.4\times10^{-2}$ $cm^2.V^{-1}.s^{-1}$, $\mu_h/\mu_e=16.5\times10^4$, **SQA-2-FPOPh$_2$**: $\mu_e=1.8\times10^{-7}$ $cm^2.V^{-1}.s^{-1}/\mu_h=5.1\times10^{-5}$ $cm^2.V^{-1}.s^{-1}$, $\mu_h/\mu_e=283$ and **SQPTZ-2-FPOPh$_2$**: $\mu_e=1.1\times10^{-4}/\mu_h=5.1\times10^{-8}$ $cm^2.V^{-1}.s^{-1}$, $\mu_h/\mu_e=4.6\times10^{-4}$). *Thus, do the SL-PhOLEDs performance follow the mobility ratio trend of the host?* Actually, the answer is clearly no. With the green Ir(ppy)$_2$acac dopant (10%), if **SIA-2-FPOPh$_2$** displays modest performance (EQE=12.9%) in accordance with the unbalanced mobility ratio, both **SQPTZ-2-FPOPh$_2$** and **SQA-2-FPOPh$_2$** surprisingly present a very high EQE of 19.3%. Tuning the ratio of dopant for **SQPTZ-2-FPOPh$_2$** even provides a very high EQE of 22.7% (8% Ir(ppy)$_2$acac) which is to date the highest EQE recorded for a SL-PhOLED (Figure 8).[24]

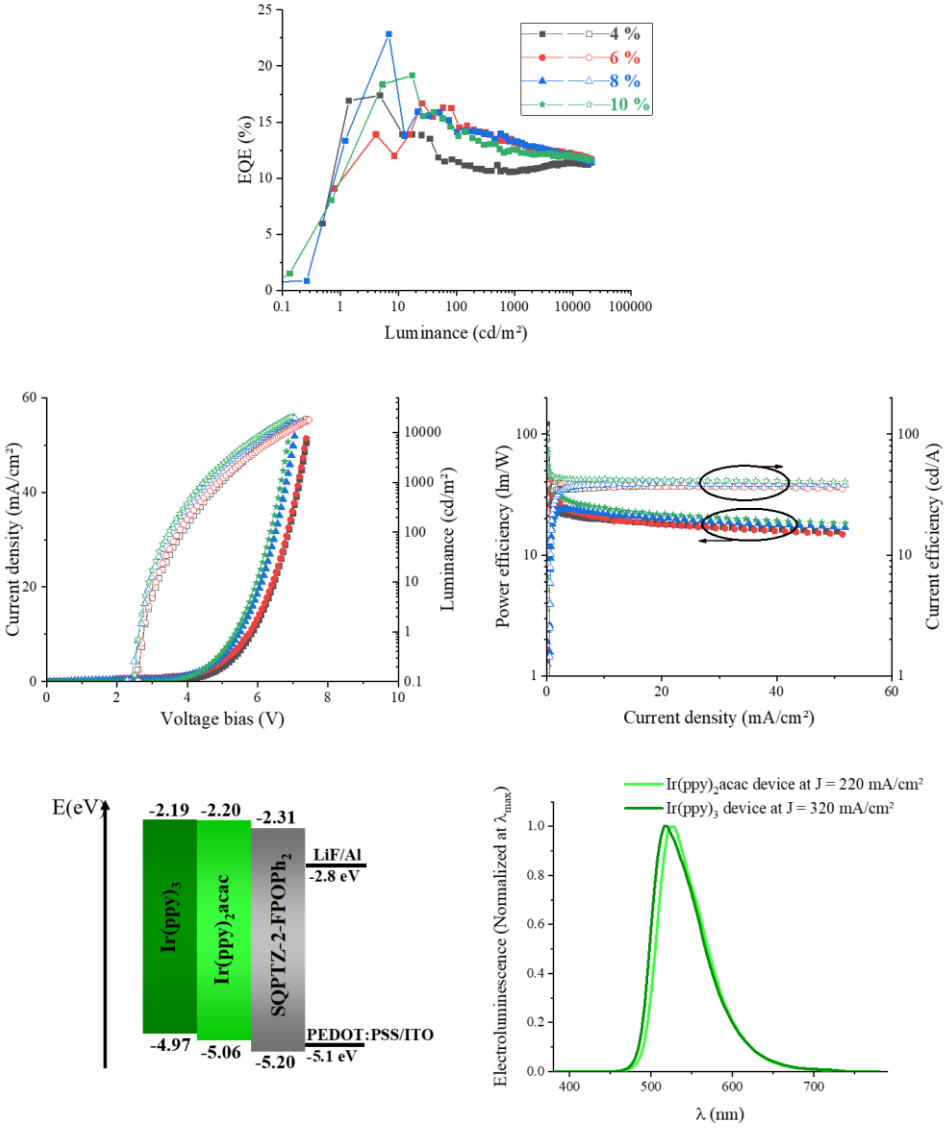

Figure 8. SL-PhOLEDs characteristics of **SQPTZ-2-FPOPh$_2$**:Ir(ppy)$_2$acac based EML at 4, 6, 8 and 10 % (Reproduced with permission from reference 24. Copyright 2022 American Chemical Society).

For the FIr6 based devices, the trend was even different increasing from **SIA-2-FPOPh$_2$**, 3.0%, **SQPTZ-2-FPOPh$_2$**, 5.8%, to **SQA-2-FPOPh$_2$** with a high EQE of 10.2%. This last value is the highest reported to date for FIr6 based SL-PhOLEDs. Thus, the different performances seemed to be directly correlated to the host/guest association. To unravel this intriguing feature, we decided, in 2022, to lead a side study in order to investigate the charge transport of the EML. Indeed, the mobility data do not reflect the influence of the iridium complex in the EML. The study was performed on **SQPTZ-2-FPOPh$_2$**. Thus, the charge transport of the EML **SQPTZ-2-FPOPh$_2$**/Ir(ppy)$_2$acac (8%), was determined providing hole and electron mobilities of 7.2×10^{-7} and 7.6×10^{-6} cm².V^{-1}.s^{-1}. This leads to a μ_e/μ_h ratio of 11, close to unity, very different to μ_e/μ_h ratio of the host (ca 2000).[24] Surprisingly, it was observed that the electron mobility is decreased and the hole mobility is increased compared to the neat host. This provides a more balanced hole/electron transport, which is a central concept to insure an excellent recombination of the charge in the centre of the EML. In this work, to highlight the specific effects induced by the dopant in the EML, another emitter, Ir(ppy)$_3$, was also

investigated. The couple **SQPTZ-2-FPOPh$_2$**/Ir(ppy)$_3$ has provided values of μ_h=7.1×10^{-8} and μ_e=1.1×10^{-5} cm^2.V^{-1}.s^{-1} giving a μ_e/μ_h of 155. This EML therefore presents a less balanced charge flow than the corresponding Ir(ppy)$_2$acac based EML, which has been related to the lower EQE of 17.9% measured for Ir(ppy)$_3$. This work has opened, in our group, a new way to correlate the performance of SL-PhOLED to the EML properties. Thus, by modifying the supramolecular arrangements and the dipole moments, the phosphor drastically modifies the transport of the host and in turn that of the EML. The evaluation of the mobilities of the EML and not only those of the host is then essential to go deeper in the understanding of the SL-PhOLEDs performance. These experiments should be now performed on different host/guest systems in order to highlight the exact effect of a specific emitter on the EML properties. This will significantly improve the knowledge and will help to design future high performance materials.

In all these works, the performance of the *D-Spiro-A* design has been evidenced by the comparison with standard compounds, 4,4′-bis(*N*-carbazolyl)-1,1′-biphenyl (CBP, HOMO/LUMO: -5.56/-2.09 eV, E_T=2.69 eV) and 1,3-bis(*N*-carbazolyl)benzene (mCP, HOMO/LUMO: -5.64/-1.90 eV, E_T=3.05 eV), usually found in high efficiency ML-PhOLEDs.[43-45] The performances measured at 10 mA/cm², in strictly identical single-layer device architecture, were both very low with EQE_{max} of 1.4% and 2.9% for CBP and mCP respectively,[24] showing the great potential of the *D-Spiro-A* design.

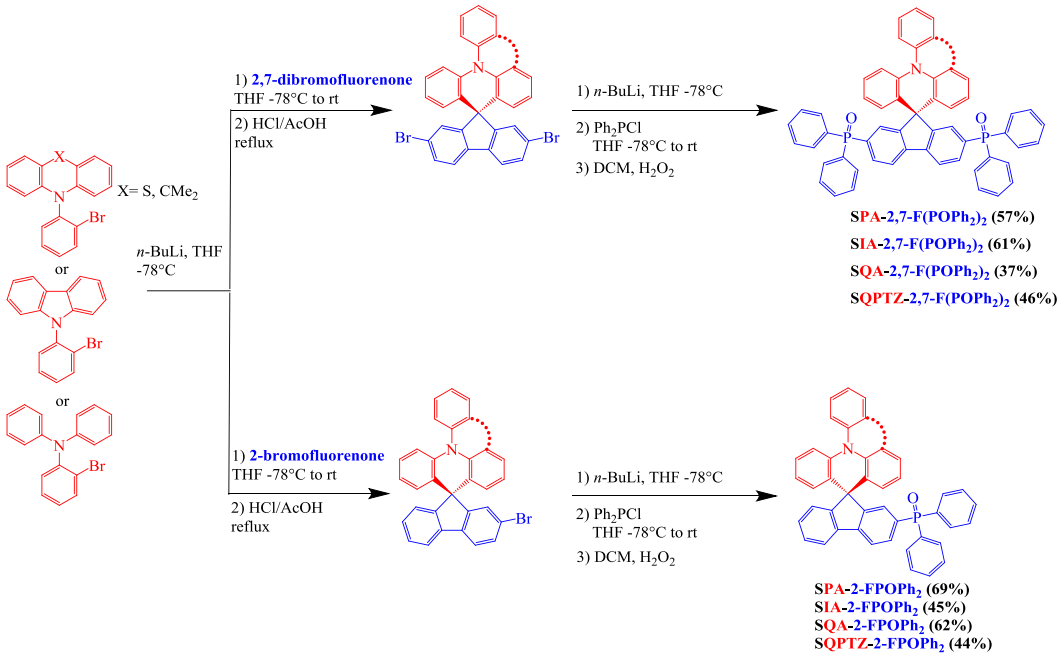

Scheme 1. Synthesis of D-*Spiro*-A host materials: A general approach

In all these works, a point has not been discussed, namely the synthetic approach. Indeed, all the molecules discussed have a common feature: they can be easily synthesized following a similar and efficient approach. To reduce the environmental footprint and for industrial applications, the synthesis of the next generation of hosts should be short and efficient, should use inexpensive starting materials and should avoid the use of rare metal catalysts. All the D-*Spiro*-A molecules considered above followed these synthetic considerations (Scheme 1). The idea was to use the fluorene building unit (substituted either at C2 or C2/C7) as a common precursor of the acceptor and to couple it to the different donor. First, a lithium–bromine exchange was performed on the 2-bromo-substituted precursor of the donor (in red, Scheme 1) followed by the nucleophilic addition reaction on the corresponding fluorenone. The next step was the intramolecular cyclization reaction to form the bromo platforms with the donor unit attached. These platforms are appealing functional scaffolds, on which

can be grafted many different molecular units. Finally, the phosphine oxides were classically introduced to reach the final compounds. This versatile approach, which can be adapted to many donor/acceptor combination, has been a strength in all our works as it has allowed synthesizing efficiently many hosts for device testing.

Other efficient D-*Spiro*-A combinations

This account is focused on the most efficient D-*Spiro*-A combination used to date, namely the association of a phenylacridine-like fragment as electron-rich unit and a fluorene/phosphine-oxides fragment as electron-poor unit. However, the literature also reported a few other combinations, of interest in the purpose of this account (Figure 8). In these examples, the E_T remains however low as substituents are grafted at C2 of fluorene, increasing in turn the π-conjugation. Indeed, these examples have been reported at the early stage of the field and before the development of spirobifluorene positional isomers (Positions C1, C3 and C4 increase the E_T) only recently reported.[16,22,27, 29, 46-49]

In 2015, the host **2,7-DiCbz-SBF-4'-POPh$_2$**, a spirobifluorene functionnalized by a diphenylphosphine oxide at C4' and by two carbazoles at C2/C7 has been reported (Figure 8).[50] This design is similar to that of **CSC**,[50] in which the acceptor is a diazafluorene. In both molecules, the donor is the same carbazole/fluorene/carbazole fragment. In **2,7-DiCbz-SBF-4'-POPh$_2$**, the C4 position of the SBF is used to avoid a dramatic drop of the E_T (2.64 eV).[26, 47, 51] The green SL-PhOLED ($Ir(ppy)_3$) possessed an interesting EQE of 13.2% and a low V_{on} of 2.4 V. The central role played by the phosphine oxide, was highlighted by comparison with **Spiro-2CBP** and **SBF-4-POPh$_2$** (Figure 8). If **Spiro-2CBP** gave a very low EQE of 0.3%, due to its bad electron transport, **SBF-4-POPh$_2$** displayed similar efficiency than **2,7-DiCbz-SBF-4'-POPh$_2$** showing the influence of the diphenylphosphine unit in the device performance. This study has shown the predominant role of the phosphine oxide fragments and has been an important starting point in our investigations in SL-PhOLEDs. **CSC** also has confirmed this feature.[52] The only difference between **CSC** and **2,7-DiCbz-SBF-4'-POPh$_2$** is the acceptor unit : diazafluorene *vs* fluorene/phosphine oxide. The E_T are almost identical for both molecules as fixed by the carbazole/fluorene/carbazole unit. The EQE of the SL-PhOLED (**CSC**:10% $Ir(ppy)_3$) is measured at 7.2%, significantly lower than that of **2,7-DiCbz-SBF-4'-POPh$_2$** (13.2%). This feature can be imputed to the absence of the phosphine oxide fragment.

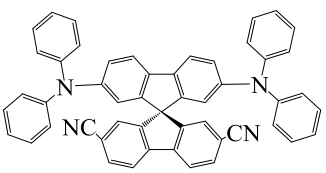

D2ACN

E_T = 2.40 eV

Ir(Mpq)$_2$(acac), 10.8%

2008

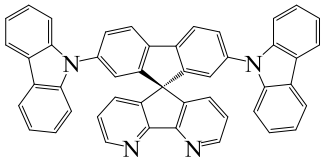

CSC

E_T = 2.65 eV

Ir(ppy)$_3$, 7.2%

Ir(ppy)$_2$(acac), 8.3%

Ir(PBI)$_2$(acac), 8.2%

Ir(TPm)$_2$(acac), 8%

2010

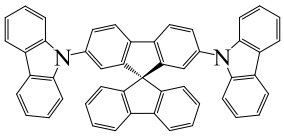

Spiro-2-CBP

E_T = 2.64 eV

Ir(ppy)$_3$, 0.3%

2015

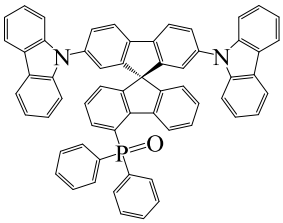

2,7-DiCbz-SBF-4-POPh$_2$

E_T = 2.64 eV

Ir(ppy)$_3$, 13.2%

2015

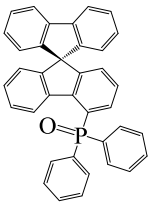

SBF-4-POPh$_2$

E_T = 2.78 eV

Ir(ppy)$_3$, 13.3%

2015

Figure 8. Examples of hosts with a D-*Spiro*-A design used SL-PhOLEDs.

D2ACN also presents a similar design with this time two cyano units at C2/C7 of the fluorene as acceptor and a diphenylamine/fluorene/diphenylamine fragment as donor. This host has been important in the history of SL-PhOLEDs as the first high efficiency red SL-PhOLED (Ir(Mpq)$_2$(acac)) overpassing 10%.[53] The depresses the LUMO energy level, -2.58 eV, was assigned to the electron-withdrawing capabilities of cyano groups,[54-56] rendering **D2ACN** well adapted to the cathode used (LiF/Al: -2.8 eV). Noted that **D2ACN** displays a balanced charge transport (2×10^{-5} cm^2 V^{-1} s^{-1} for μ_e and 4.7×10^{-5} cm^2 V^{-1} s^{-1} for μ_h). As far as we known, this work is still the highest performance of red SL-PhOLEDs (with a single host).

Conclusions

The D-*Spiro*-A molecular design has appeared, in recent years, as one of the most efficient design in the field of SL-PhOLED and has already provided key results. The combination discussed herein is based on phenylacridine-like fragments as donor and fluorene/phosphine oxide as acceptor. This combination is to date the most efficient reported for SL-PhOLEDs. The advantages of this design are manifold and mainly based on the presence of the spiro-carbon allowing (i) to separate the HOMO and LUMO and then easily controlling their energy levels and (ii) to reach good thermal and morphological properties. In this design, the most difficult parameter to control is undoubtedly the charge transport. Indeed, a small structural modification drastically modifies both the electron and the hole mobility. However, in simplified SL-PhOLEDs, this charge transport should be as balance as possible to optimize the exciton formation in the EML. This is a crucial consideration in SL-PhOLEDs, far more important than in ML-PhOLEDs. Recently, important insights have been made on the concept of ambipolarity for SL-PhOLED application and the D-*Spiro*-A design is at the origin of these advances. When measuring the electron and hole mobility, the whole EML should be considered since the presence of the emitter, despite in small amount, drastically modifies the charge transport compared to the host alone.

There is no doubt that other advances will be made with the D-*Spiro*-A design in the field of SL-PhOLEDs. Finding relevant Donor/Acceptor combinations will be the key. This account has focused on fluorene/diphosphine oxide as acceptor and it is clear that phosphine oxide units are significantly involved in the high performance reached. These fragments have also revealed unexpected photophysical properties, for example for **SPA-2,7-F(POPh$_2$)$_2$**, the simultaneous occurrence of emission from intermolecular and intramolecular charge-transfer excited states has been reported when incorporated as emitter in an OLED.[42, 57] Indeed, the D-*Spiro*-A design has also been advantageously used in the elaboration of fluorophores displaying, thanks to a short π-conjugated pathway, an emission at short wavelengths (highly necessary in the field of OLEDs).[58]

However, in the field of hosts for SL-PhOLEDs, other acceptors should be tested, grafted or not on a fluorene backbone. Until now, only very few examples have been reported,[53] but this direction appears interesting to manage the electron flow. The incorporation of acceptor fused in the fluorene such as reported with a benzimidazole fragment by Liao et al in 2018 appears particularly promising.[59] Acridophosphine oxides also appear as a relevant strategy to introduce electron-accepting functionalities while keeping a high E_T.[60] Finally, increasing the E_T value (compared to the hosts described in this account) should also be considered in order to use deep blue phosphorescent emitters. For that purpose, the fluorene should be absolutely removed in order to shorten the π-conjugated pathway. This may open promising possibilities to design high E_T D-*Spiro*-A hosts.

Supporting Information

A table gathering the devices performance presented in this account is provided.

Acknowledgments

The authors highly thank all the members from the group, which have been involved at different stages of the '*Single-layer'* project (Dr Fabien Lucas, Clément Brouillac, Denis Ari, Dr Cassandre Quinton). Colaborators from other groups are also highly thank, namely Dr Emmanuel Jacques, Dr Denis Tondelier and Bernard Geffroy. We warmly thank the ANR (SPIROQUEST, n°19-CE05-0024) for financial support of the 'Single-Layer' project, the Région Bretagne (DIADEM project) and the Agence de l'Environnement et de la Maitrîse de l'Energie (ADEME) for PhD grant (FL and CB respectively). Dr Bruno Lafitte (ADEME) is particularly thanked. This work was granted access to the HPC resources of CINES under the allocation 2022 (Project N°AD0100805032R) awarded by GENCI. The authors thank Dr J.F. Bergamini (Rennes) for the TOC material.

Received: ((will be filled in by the editorial staff))

Published online: ((will be filled in by the editorial staff)).

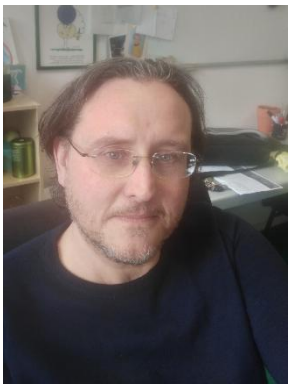

Cyril Poriel is CNRS Research Director at Institut des Sciences Chimiques de Rennes, France. His main research interest deals with the design of π-conjugated molecular architectures for Organic Electronics. He is interested in the design of blue emitting fluorophores for OLEDs, high-triplet hosts for phosphorescent OLEDs, electron deficient semiconductors for OFETs and nanohoops. These works have led to more than 120 publications.

Joëlle Rault-Berthelot is CNRS Research Director at Institut des Sciences Chimiques de Rennes. She has more than 40 years experience in electrochemistry of π-conjugated systems for organic electronic, which have led to ca 200 publications.

References

(1) Poriel, C.; Rault-Berthelot, J., Blue Single-Layer Organic Light-Emitting Diodes Using Fluorescent Materials: A Molecular Design View Point. *Adv. Funct. Mat.* **2020,** *30*, 1910040.

(2) Poriel, C.; Rault- Berthelot, J., Designing Host Materials for the Emissive Layer of Single- Layer Phosphorescent Organic Light- Emitting Diodes: Toward Simplified Organic Devices. *Adv. Funct. Mater.* **2021,** *31*, 2010547.

(3) Fan, C.; Chen, Y.; Liu, Z.; Jiang, Z.; Zhong, C.; Ma, D.; Qin, J.; Yang, C., Tetraphenylsilane derivatives spiro-annulated by triphenylamine/carbazole with enhanced HOMO energy levels and glass transition temperatures without lowering triplet energy: host materials for efficient blue phosphorescent OLEDs *J. Mater. Chem. C* **2013,** *1*, 463-469.

(4) Thiery, S.; Tondelier, D.; Geffroy, B.; Jeannin, O.; Rault-Berthelot, J.; Poriel, C., Modulation of the Physicochemical Properties of Donor–Spiro–Acceptor Derivatives through Donor Unit Planarisation: Phenylacridine versus Indoloacridine—New Hosts for Green and Blue Phosphorescent Organic Light-Emitting Diodes (PhOLEDs). *Chem. Eur. J.* **2016,** *22*, 10136-10149.

(5) Romain, M.; Quinton, C.; Tondelier, D.; Geffroy, B.; Jeannin, O.; Rault-Berthelot, J.; Poriel, C., Thioxanthene and dioxothioxanthene dihydroindeno[2,1-b]fluorenes: synthesis, properties and applications in green and sky blue phosphorescent OLEDs. *J. Mater. Chem. C* **2016,** *4*, 1692-1703.

(6) Poriel, C.; Rault-Berthelot, J.; Thiery, S.; Quinton, C.; Jeannin, O.; Biapo, U.; Geffroy, B.; Tondelier, D., 9H-Quinolino[3,2,1-k]phenothiazine: A New Electron-Rich Fragment for Organic Electronics. *Chem. Eur. J.* **2016,** *22*, 17930-17935.

(7) Romain, M.; Tondelier, D.; Jeannin, O.; Geffroy, B.; Rault-Berthelot, J.; Poriel, C., Properties modulation of organic semi-conductors based on a donor-spiro-acceptor (D-spiro-A) molecular design: new host materials for efficient sky-blue PhOLEDs. *J. Mater. Chem. C* **2015,** *3*, 97010-97014.

(8) Romain, M.; Tondelier, D.; Geffroy, B.; Jeannin, O.; Jacques, E.; Rault-Berthelot, J.; Poriel, C., Donor/Acceptor Dihydroindeno[1,2-a]fluorene and Dihydroindeno[2,1-b]fluorene: Towards New Families of Organic Semiconductors. *Chem. Eur. J.* **2015,** *21*, 9426–9439,.

(9) Zhu, X.-D.; Zhang, Y.-L.; Yuan, Y.; Zheng, Q.; Yu, Y.-J.; Li, Y.; Jiang, Z.-Q.; Liao, L.-S., Incorporating a tercarbazole donor in a spiro-type host material for efficient RGB phosphorescent organic light-emitting diodes. *J. Mater. Chem. C* **2019,** *7*, 6714-6720.

(10) Khan, A.; Wang, Y.-K.; Huang, C.-C.; Kumar, S.; Fung, M.-K.; Jiang, Z.-Q.; Liao, L.-S., Donor-spiro-acceptor architecture for green thermally activated delayed fluorescence (TADF) emitter. *Org. Electron.* **2020,** *77*, 105520.

(11) Sharma, N.; Maciejczyk, M.; Hall, D.; Li, W.; Liégeois, V.; Beljonne, D.; Olivier, Y.; Robertson, N.; Samuel, I. D. W.; Zysman-Colman, E., Spiro-Based Thermally Activated Delayed Fluorescence Emitters with Reduced Nonradiative Decay for High-Quantum-Efficiency, Low-Roll-Off, Organic Light-Emitting Diodes. *ACS Appl. Mater. Interfaces* **2021,** *13*, 44628-44640.

(12) Nasu, K.; Nakagawa, T.; Nomura, H.; Lin, C.-J.; Cheng, C.-H.; Tseng, M.-R.; Yasuda, T.; Adachi, C., A highly luminescent spiro-anthracenone-based organic light-emitting diode exhibiting thermally activated delayed fluorescence *Chem. Commun.* **2013,** *49*, 10385-10387.

(13) Wang, Y. K.; Huang, C. C.; Ye, H.; Zhong, C.; Khan, A.; Yang, S. Y.; Fung, M. K.; Jiang, Z. Q.; Adachi, C.; Liao, L. S., Through Space Charge Transfer for Efficient Sky- Blue Thermally Activated Delayed Fluorescence (TADF) Emitter with Unconjugated Connection. *Adv. Opt. Mater.* **2019,** *8*, 1901150.
(14) Peng, C. C.; Yang, S. Y.; Li, H. C.; Xie, G. H.; Cui, L. S.; Zou, S. N.; Poriel, C.; Jiang, Z. Q.; Liao, L. S., Highly Efficient Thermally Activated Delayed Fluorescence via an Unconjugated Donor-Acceptor System Realizing EQE of Over 30%. *Adv. Mater.* **2020,** *32*, 2003885.
(15) Franca, L. G.; Long, Y.; Li, C.; Danos, A.; Monkman, A., The Critical Role of nπ* States in the Photophysics and Thermally Activated Delayed Fluorescence of Spiro Acridine-Anthracenone. *J. Phys. Chem. Lett.* **2021,** *12*, 1490-1500.
(16) Sicard, L.; Quinton, C.; Peltier, J.-D.; Tondelier, D.; Geffroy, B.; Biapo, U.; Métivier, R.; Jeannin, O.; Rault-Berthelot, J.; Poriel, C., Spirobifluorene Regioisomerism: A Structure–Property Relationship Study. *Chem. Eur. J.* **2017,** *23*, 7719-7723.
(17) Lucas, F.; Ibraikulov, O. A.; Quinton, C.; Sicard, L.; Heiser, T.; Tondelier, D.; Geffroy, B.; Leclerc, N.; Rault-Berthelot, J.; Poriel, C., Spirophenylacridine-2,7-(diphenylphosphineoxide)-fluorene: A Bipolar Host for High-Efficiency Single-Layer Blue Phosphorescent Organic Light-Emitting Diodes. *Adv. Opt. Mater.* **2020,** *8*, 1901225.
(18) Lee, J.-H.; Chen, C.-H.; Lee, P.-H.; Lin, H.-Y.; Leung, M.-k.; Chiu, T.-L.; Lin, C.-F., Blue organic light-emitting diodes: current status, challenges, and future outlook. *J. Mater. Chem. C* **2019,** *7*, 5874-5888.
(19) Wang, Y.; Yun, J. H.; Wang, L.; Lee, J. Y., High Triplet Energy Hosts for Blue Organic Light-Emitting Diodes. *Adv. Funct. Mater.* **2020,** *31*, 2008332.
(20) Monkman, A., Why Do We Still Need a Stable Long Lifetime Deep Blue OLED Emitter? *ACS Appl. Mater. Interfaces* **2022,** *14*, , 20463–20467.
(21) Lucas, F.; Quinton, C.; Fall, S.; Heiser, T.; Tondelier, D.; Geffroy, B.; Leclerc, N.; Rault-Berthelot, J.; Poriel, C., Universal host materials for red, green and blue high-efficiency single-layer phosphorescent organic light-emitting diodes. *J. Mater. Chem. C* **2020,** *8*, 16354-16367.
(22) Poriel, C.; Quinton, C.; Lucas, F.; Rault- Berthelot, J.; Jiang, Z. Q.; Jeannin, O., Spirobifluorene Dimers: Understanding How The Molecular Assemblies Drive The Electronic Properties. *Adv. Funct. Mater.* **2021**, 2104980.
(23) Thiery, S.; Tondelier, D.; Declairieux, C.; Geffroy, B.; Jeannin, O.; Métivier, R.; Rault-Berthelot, J.; Poriel, C., 4-Pyridyl-9,9′-spirobifluorenes as Host Materials for Green and Sky-Blue Phosphorescent OLEDs. *J. Phys. Chem. C* **2015,** *119*, 5790–5805.
(24) Lucas, F.; Brouillac, C.; Fall, S.; Zimmerman, N.; Tondelier, D.; Geffroy, B.; Leclerc, N.; Heiser, T.; Lebreton, C.; Jacques, E.; Quinton, C.; Rault-Berthelot, J.; Poriel, C., Simplified Green-Emitting Single-Layer Phosphorescent Organic Light-Emitting Diodes with an External Quantum Efficiency > 22%. *Chem. Mater.* **2022,** *34*, 8345–8355.
(25) Hsu, F.-M.; Chien, L.-J.; Chen, K.-T.; Li, Y.-Z.; Liu, S.-W., High morphology stability and ambipolar transporting host for use in blue phosphorescent single-layer organic light-emitting diodes. *Org. Electron.* **2014,** *15*, 3327-3332.
(26) Poriel, C.; Sicard, L.; Rault-Berthelot, J., New generations of spirobifluorene regioisomers for organic electronics: tuning electronic properties with the substitution pattern. *Chem. Comm.* **2019,** *55*, 14238-14254.
(27) Wang, Q.; Lucas, F.; Quinton, C.; Qu, Y.-K.; Rault-Berthelot, J.; Jeannin, O.; Yang, S.-Y.; Kong, F.-C.; Kumar, S.; Liao, L.-S.; Poriel, C.; Jiang, Z.-Q., Evolution of pure hydrocarbon hosts: simpler structure, higher performance and universal application in RGB phosphorescent organic light-emitting diodes. *Chem. Sci.* **2020,** *11*, 4887-4894.
(28) Sicard, L. J.; Li, H.-C.; Wang, Q.; Liu, X.-Y.; Jeannin, O.; Rault-Berthelot, J.; Liao, L.-S.; Jiang, Z.-Q.; Poriel, C., C1-Linked Spirobifluorene Dimers: Pure Hydrocarbon Hosts for High-Performance Blue Phosphorescent OLEDs. *Angew. Chem. Int. Ed.* **2019,** *58*, 3848-3853.
(29) Poriel, C.; Rault-Berthelot, J., Pure Hydrocarbons: An Efficient Molecular Design Strategy for the Next Generation of Host Materials for Phosphorescent Organic Light-Emitting Diodes. *Acc. Mater. Res.* **2022,** *3*, 379-390.

(30) Wu, C.; Wang, B.; Wang, Y.; Hu, J.; Jiang, J.; Ma, D.; Wang, Q., A universal host material with a simple structure for monochrome and white phosphorescent/TADF OLEDs. *J. Mater. Chem. C* **2019,** *7*, 558-566.
(31) Gao, K.; Liu, K.; Li, X.-L.; Cai, X.; Chen, D.; Xu, Z.; He, Z.; Li, B.; Qiao, Z.; Chen, D.; Cao, Y.; Su, S.-J., An ideal universal host for highly efficient full-color, white phosphorescent and TADF OLEDs with a simple and unified structure. *J. Mater. Chem. C* **2017,** *5*, 10406-10416.
(32) Méhes, G.; Nomura, H.; Zhang, W.; Nakagawa, T.; Adachi, C., Enhanced Electroluminescence Efficiency in a Spiro-Acridine Derivative through Thermally Activated Delayed Fluorescence *Angew. Chem. Int. Ed.* **2012,** *51*, 11311-11315.
(33) Zou, S. N.; Chen, X.; Yang, S. Y.; Kumar, S.; Qu, Y. K.; Yu, Y. J.; Fung, M. K.; Jiang, Z. Q.; Liao, L. S., Efficient Violet Organic Light- Emitting Diodes with CIEy of 0.02 Based on Spiro Skeleton. *Adv. Opt. Mater.* **2020,** *8*, 2001074.
(34) Zhang, Y.-X.; Ding, L.; Liu, X.-Y.; Chen, H.; Ji, S.-J.; Liao, L.-S., Spiro-fused N-phenylcarbazole-based host materials for blue phosphorescent organic light-emitting diodes. *Org. Electron.* **2015,** *20*, 112-118.
(35) Zang, C.; Peng, X.; Wang, H.; Yu, Z.; Zhang, L.; Xie, W.; Zhao, H., Efficient multilayer and single layer phosphorescent organic light-emitting devices using a host with balanced bipolar transporting properties and appropriate energy level. *Org. Electron.* **2017,** *50*, 106-114.
(36) Quinton, C.; Sicard, L.; Jeannin, O.; Vanthuyne, N.; Poriel, C., Confining Nitrogen Inversion to Yield Enantiopure Quinolino[3,2,1-k]Phenothiazine Derivatives. *Adv. Funct. Mat.* **2018,** *28*, 1803140-1803147.
(37) Khan, A.; Chen, X.; Kumar, S.; Yang, S.-Y.; Yu, Y.-J.; Luo, W.; Jiang, Z.-Q.; Fung, M.-K.; Liao, L.-S., Spiro-type host materials with rigidified skeletons for RGB phosphorescent OLEDs. *J. Mater. Chem. C* **2020,** *8*, 12470-12477.
(38) Seo, J.-A.; Gong, M. S.; Lee, J. Y., Thermally stable indoloacridine type host material for high efficiency blue phosphorescent organic light-emitting diodes. *Org. Electron.* **2014,** *15*, 3773-3779.
(39) Yang, S. Y.; Feng, Z. Q.; Fu, Z.; Zhang, K.; Chen, S.; Yu, Y. J.; Zou, B.; Wang, K.; Liao, L. S.; Jiang, Z. Q., Highly Efficient Sky-Blue pi-Stacked Thermally Activated Delayed Fluorescence Emitter with Multi-Stimulus Response Properties. *Angew Chem Int Ed Engl* **2022**, e202206861.
(40) Lucas, F.; Tondelier, D.; Geffroy, B.; Heiser, T.; Ibraikulov, O. A.; Quinton, C.; Brouillac, C.; Leclerc, N.; Rault-Berthelot, J.; Poriel, C., Quinolinophenothiazine as Electron Rich Fragment for RGB Single-Layer Phosphorescent Organic Light-Emitting Diodes. *Mater. Chem. Front.* **2021,** *5*, 8066-8077.
(41) *unpublished results*.
(42) Tourneur, P.; Lucas, F.; Brouillac, C.; Quinton, C.; Lazzaroni, R.; Olivier, Y.; Viville, P.; Poriel, C.; Cornil, J., When Poor Light- Emitting Spiro Compounds in Solution Turn into Emissive Pure Layers in Organic Light- Emitting Diodes: The Key Role of Phosphine Substituents. *Adv. Photonics Res.* **2022**, 2200124.
(43) Helander, M. G.; Wang, Z. B.; Qiu, J.; Greiner, M. T.; Puzzo, D. P.; Liu, Z. W.; Lu, Z. H., Chlorinated Indium Tin Oxide Electrodes with High Work Function for Organic Device Compatibility. *Science* **2011,** *332*, 944-947.
(44) Wang, Z. B.; Helander, M. G.; Qiu, J.; Puzzo, D. P.; Greiner, M. T.; Liu, Z. W.; Lu, Z. H., Highly simplified phosphorescent organic light emitting diode with >20% external quantum efficiency at >10,000cd/m2. *App. Phys. Lett.* **2011,** *98*, 073310.
(45) Ma, B.; Djurovich, P. I.; Garon, S.; Alleyne, B.; Thompson, M. E., Platinum Binuclear Complexes as Phosphorescent Dopants for Monochromatic and White Organic Light-Emitting Diodes. *Adv. Funct. Mater.* **2006,** *16*, 2438-2446.
(46) Kong, F. C.; Zhang, Y. L.; Quinton, C.; McIntosh, N.; Yang, S. Y.; Rault-Berthelot, J.; Lucas, F.; Brouillac, C.; Jeannin, O.; Cornil, J.; Jiang, Z. Q.; Liao, L. S.; Poriel, C., Pure Hydrocarbon Materials as Highly Efficient Host for White Phosphorescent Organic Light-Emitting Diodes: A New Molecular Design Approach. *Angew Chem Int Ed Engl* **2022,** *61*, e202207204.
(47) Quinton, C.; Thiery, S.; Jeannin, O.; Tondelier, D.; Geffroy, B.; Jacques, E.; Rault-Berthelot, J.; Poriel, C., Electron-Rich 4-Substituted Spirobifluorenes: Toward a New Family of High Triplet Energy Host Materials for High-Efficiency Green and Sky Blue Phosphorescent OLEDs. *ACS Appl. Mater. Interfaces.* **2017,** *9*, 6194–6206.

(48) Sicard, L.; Quinton, C.; Lucas, F.; Jeannin, O.; Rault-Berthelot, J.; Poriel, C., 1-Carbazolyl Spirobifluorene: Synthesis, Structural, Electrochemical, and Photophysical Properties. *J. Phys. Chem. C* **2019,** *123*, 19094-19104.
(49) Poriel, C.; Rault-Berthelot, J.; Jiang, Z.-Q., Are pure hydrocarbons the future of host materials for blue phosphorescent organic light-emitting diodes? *Mater. Chem. Front.* **2022,** *6*, 1246-1252.
(50) Thiery, S.; Tondelier, D.; Geffroy, B.; Jacques, E.; Robin, M.; Métivier, R.; Jeannin, O.; Rault-Berthelot, J.; Poriel, C., Spirobifluorene-2,7-dicarbazole-4′-phosphine Oxide as Host for High-Performance Single-Layer Green Phosphorescent OLED Devices. *Org. Lett.* **2015,** *17*, 4682-4685.
(51) Poriel, C.; Rault-Berthelot, J., Structure–property relationship of 4-substituted-spirobifluorenes as hosts for phosphorescent organic light emitting diodes: an overview. *J. Mater. Chem. C* **2017,** *5*, 3869-3897
(52) Hung, W.-Y.; Wang, T.-C.; Chiu, H.-C.; Chen, H.-F.; Wong, K.-T., A spiro-configured ambipolar host material for impressively efficient single-layer green electrophosphorescent devices. *Phys. Chem. Chem. Phys.* **2010,** *12*, 10685-10687.
(53) Hung, W.-Y.; Tsai, T.-C.; Ku, S.-Y.; Chi, L.-C.; Wong, K.-T., *Phys. Chem. Chem. Phys.* **2008,** *10*, 5822-5825.
(54) Bebiche, S.; Cisneros-Perez, P.; Mohammed-Brahim, T.; Harnois, M.; Rault-Berthelot, J.; Poriel, C.; Jacques, E., Influence of the gate bias stress on the stability of n-type Organic Field-Effect Transistors based on Dicyanovinylenes-Dihydroindenofluorene semiconductors. *Mater. Chem. Front.* **2018,** *2*, 1631-1641.
(55) Peltier, J.-D.; Heinrich, B.; Donnio, B.; Jacques, E.; Rault-Berthelot, J.; Poriel, C., Electron-Deficient Dihydroindaceno-Dithiophene Regioisomers for n-Type Organic Field-Effect Transistors. *ACS Appl. Mater. Interfaces* **2017,** *9*, 8219-8232.
(56) Peltier, J.-D.; Heinrich, B.; Donnio, B.; Jeannin, O.; Rault-Berthelot, J.; Jacques, E.; Poriel, C., N-Cyanoimine as an electron-withdrawing functional group for organic semiconductors: example of dihydroindacenodithiophene positional isomers. *J. Mater. Chem. C* **2018,** *6*, 13197-13210.
(57) Tourneur, P.; Lucas, F.; Quinton, C.; Olivier, Y.; Lazzaroni, R.; Viville, P.; Cornil, J.; Poriel, C., White-light electroluminescence from a layer incorporating a single fully-organic spiro compound with phosphine oxide substituents. *J. Mater. Chem. C* **2020,** *8*, 14462-14468.
(58) Brouillac, C.; Shen, W.-S.; Rault-Berthelot, J.; Jeannin, O.; Quinton, C.; Jiang, Z.-Q.; Poriel, C., Spiro-configured dibenzosuberene compounds as deep-blue emitters for organic light-emitting diodes with a CIEy of 0.04. *Mater. Chem. Front.* **2022,** *6*, 1803-1813.
(59) Chen, W.-C.; Yuan, Y.; Zhu, Z.-L.; Ni, S.-F.; Jiang, Z.-Q.; Liao, L.-S.; Wong, F.-L.; Lee, C.-S., A novel spiro-annulated benzimidazole host for highly efficient blue phosphorescent organic light-emitting devices. *Chem. Comm.* **2018,** *54*, 4541-4544.
(60) Zhao, X.-H.; Duan, C.-B.; Ma, X.; Zou, G.-D.; Zhang, J.; Xu, H.; Xie, L.-H.; Yuan, S.-D.; Yang, Y.-J.; Huang, W., The coordinated tunning optical, electrical and thermal properties of spiro-configured phenyl acridophopsphine oxide and sulfide for host materials. *Org. Electron.* **2021,** *95*, 106193.